



# Study on Seismic Performance and Application of L-shaped Concrete-filled Steel Tube Column

Shiqi Jiang

School of Civil Engineering, Chang'an University, Xi'an, China

E-mail: 843273299@qq.com

**Abstract.** In rural residential housing, there are issues such as limited homestead land area, leading to insufficient actual indoor usable space. Steel tube concrete special-shaped columns have good load-bearing capacity, occupy a small footprint, which can solve the problem of protruding indoor column bases. They also have good assembly performance. Therefore, research on the seismic performance of steel tube concrete special-shaped columns is of great significance. In order to study the seismic performance of L-shaped concrete-filled steel tube columns and promote their applications in buildings, the hysteretic curve and skeleton curve were studied by calculation and analysis with ABAQUS software, taking the axial compression ratio and steel tube thickness as parameters. Moreover, the seismic calculation of the whole frame structure was carried out with ETABS software in conjunction the actual building structure design. Results show that L-shaped concrete-filled steel tube columns have the advantages of simple construction and high assembly performance. They have application potential in improving the seismic performance of buildings, so they can be widely applied in rural buildings.

**Keywords:** L-shaped concrete-filled steel tube column; seismic performance; finite element; frame structure.

## 1 Introduction

The text discusses the high seismic performance requirements for buildings in Yunnan Province, China, especially in rural areas where houses often face issues like limited usable indoor space due to small plot sizes. To address these challenges, special attention is given to the use of steel tube reinforced concrete columns with unique shapes, particularly L-shaped columns, which offer high load-bearing capacity and can effectively reduce the intrusion of column bases into living spaces, making them a promising solution for rural architecture.

Several researchers have contributed to this field. Hu Xiangyi [1] studied the seismic performance and damping effects of square steel tube reinforced concrete columns in high-intensity earthquake zones. Zhou Yujing [2] conducted seismic performance studies on L-shaped steel tube reinforced concrete column joints using finite element anal-

ysis. Zhang Juan [3] demonstrated the seismic resistance and energy dissipation capabilities of L-shaped steel tube reinforced concrete columns through experiments and finite element calculations, considering parameters like slenderness ratio, steel content, and axial compression ratio. Zhao Bingzhen [4] researched the performance of SCFST (steel-concrete-filled steel tube) column structures in high-rise residential buildings under seismic loads, providing valuable insights for practical engineering applications. Wang Shuai [5] conducted pseudo-static tests on a steel tube reinforced concrete column frame and performed elasto-plastic numerical analysis on the frame using finite element methods. Rosario Monteori [6] conducted experimental and analytical research on the neutral energy of circular steel tube concrete under cyclic bending. Pronnoy Bhat [7] studied the compressive performance of double-layer steel tube concrete columns.

The text also highlights that, due to varying levels of design and construction quality, many rural buildings in Yunnan suffer significant damage in earthquakes, leading to substantial property loss [8-9]. However, there has been a lack of research on steel tube reinforced concrete columns specifically suited for rural architecture. Using ABAQUS, a finite element model was developed, applying constant axial and cyclic horizontal forces, to study the seismic performance of L-shaped steel tube reinforced concrete columns. This study includes the analysis of displacement load skeleton curves and hysteresis curves. Additionally, the practicality of these columns in Yunnan's rural architecture is evaluated by conducting seismic calculations on building structural frames using ETABS.

## 2 Overview of the Finite Element Model

Based on the actual needs of rural and town architecture, an L-shaped steel tube concrete column without stiffening measures has been designed. The external steel tube uses Q235 steel, and the interior is filled with C30 concrete. The width of the column limbs of the L-shaped column is set at 200 mm, equal to the actual wall thickness in rural and town buildings. For convenience in finite element calculations, a 1:2 scale model is established, thus the width of the column limbs is 100 mm, and the length is 200 mm, with each specimen having a height of 900 mm.

The finite element software ABAQUS is used for numerical simulation analysis of the specimens. The steel material uses a five-stage strain-stress relationship model [10], and the concrete, according to reference [11], uses a plastic damage model (CDP model) to define the concrete material. The steel tube uses a quadrilateral reduced integration shell element (S4R), and the concrete uses a hexahedral reduced integration solid element (C3D8R). In the model, the steel tube and concrete are in face-to-face contact, with normal contact using a 'hard' contact. The steel tube uses a tied constraint to simulate welding action, and the discretization method chosen is node-to-surface. To effectively simulate the force situation of the L-shaped steel tube concrete column under earthquake load, the model uses displacement control, applying constant axial force and horizontal cyclic force. The finite element model of the special-shaped column is shown in Figure 1."

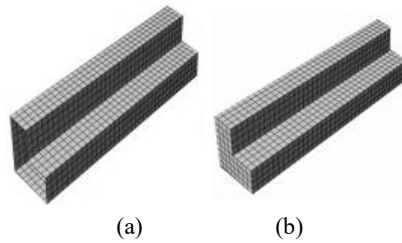


**Fig. 1.** Finite Element Model of the Special-Shaped Column(a)Finite Element Model of the Steel Tube; (b) Finite Element Model of the Internally Poured Concrete.

### 3 Seismic Performance Parameter Analysis of Special-Shaped Columns

#### 3.1 Influence of Axial Compression Ratio

Limiting the axial compression ratio can control the ductility of a structure. In some areas of Yunnan Province, the seismic intensity reaches up to degree 9. According to GB 50011—2010 "Code for Seismic Design of Buildings" (2016 edition), for frame structures with a height  $\leq 24$  m and a seismic grade of level one, the limit of the axial compression ratio for columns is 0.65. The axial compression ratio limit for steel tube reinforced concrete columns can be appropriately reduced by 0.05. Therefore, the axial compression ratios studied are 0.6, 0.5, 0.4, and 0.3.

The analysis results of the hysteresis curves, as shown in Figure 2, reveal that at low input displacements, the hysteresis curves for different axial compression ratios are diagonal lines passing through the origin, indicating elastic deformation of the L-shaped steel tube reinforced concrete columns. As the axial compression ratio decreases, the hysteresis curves become more regular and fuller. At axial compression ratios of 0.5 and 0.6, the hysteresis curves are irregular, indicating poor ductility of the specimens. In contrast, at axial compression ratios of 0.3 and 0.4, the hysteresis curves form fuller shuttle shapes, suggesting good seismic performance and ability to meet seismic demands.

Figure 3 shows the displacement-load relationship skeleton curves of the L-shaped steel tube reinforced concrete columns under different axial compression ratios, which are S-shaped. When the displacement load increases from 0 mm to 4 mm, the skeleton curve is a diagonal straight line passing through the origin, indicating elastic deformation of the L-shaped columns under different axial compression ratios. As the displacement load continues to increase to 6 mm, the larger the axial compression ratio, the smaller the inclination angle of the skeleton curve, the smaller the peak load, indicating elasto-plastic deformation of the L-shaped columns. When the displacement load increases to 10 mm, the larger the axial compression ratio, the steeper the skeleton curve, and the smaller the load corresponding to the limit displacement. This indicates that L-shaped columns with axial compression ratios of 0.3 or 0.4 have better ductility, seismic performance, stiffness, and load-bearing capacity compared to those with axial compression ratios of 0.5 or 0.6.

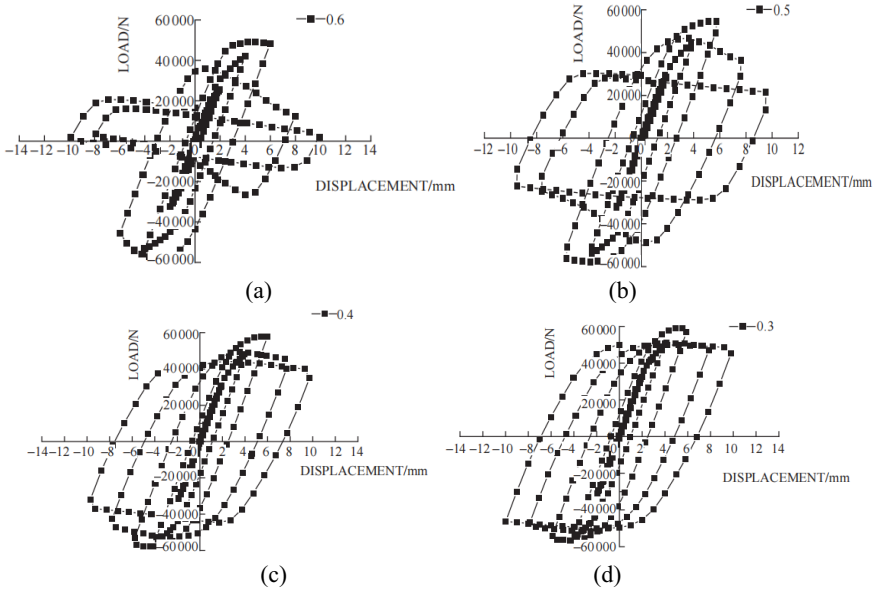


**Fig. 2.** Hysteresis Curves for Different Axial Compression Ratios(a)Hysteresis curve for an axial compression ratio of 0.6; (b) Hysteresis curve for an axial compression ratio of 0.5; (c) Hysteresis curve for an axial compression ratio of 0.4; (d) Hysteresis curve for an axial compression ratio of 0.3.

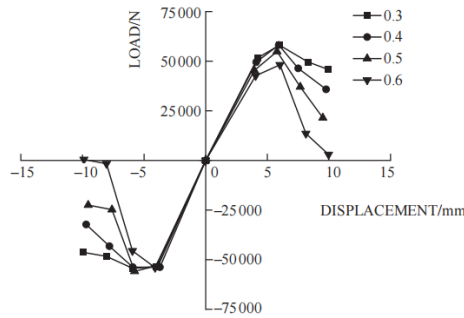


**Fig. 3.** Skeleton Curves for Different Axial Compression Ratios.

### 3.2 Steel Thickness Influence

Considering issues such as remote rural locations and high construction material transportation costs, controlling the steel thickness can effectively manage economic costs. Therefore, the seismic performance of steel tube concrete L-shaped columns was analyzed with steel thickness parameters of 2 mm, 3 mm, 4 mm, and 5 mm.

Figure 4 shows the hysteresis curves of L-shaped columns with different steel thicknesses. When subjected to initial displacement loads, the hysteresis curves of L-shaped

columns with different steel thicknesses are straight lines passing through the origin. The greater the steel thickness, the steeper the slope of the line, indicating a higher initial stiffness, and the L-shaped columns undergo elastic deformation. When the steel thickness is 3 mm, 4 mm, or 5 mm, the hysteresis curves of L-shaped columns are hysteresis-shaped, indicating better seismic performance. As the steel thickness increases, the peak loads and the area under the hysteresis curve also increase, indicating better seismic performance.

Figure 5 shows the load-displacement relationships and skeleton curves of steel tube concrete L-shaped columns with different steel thicknesses. They all exhibit an "S" shape. During the initial displacement load phase, L-shaped columns with different steel thicknesses undergo elastic deformation, and the greater the steel thickness, the higher the initial stiffness and load-bearing capacity of the specimens. As the load increases, the differences in the skeleton curves for different steel thicknesses become more pronounced. It can be observed that a greater steel tube thickness results in stronger column ductility and seismic performance, especially with significantly different ultimate load-bearing capacities. When the steel tube wall thickness increases from 2 mm to 3 mm, 4 mm, and 5 mm, the corresponding peak loads increase by 30.4%, 54.8%, and 82.0%, respectively.

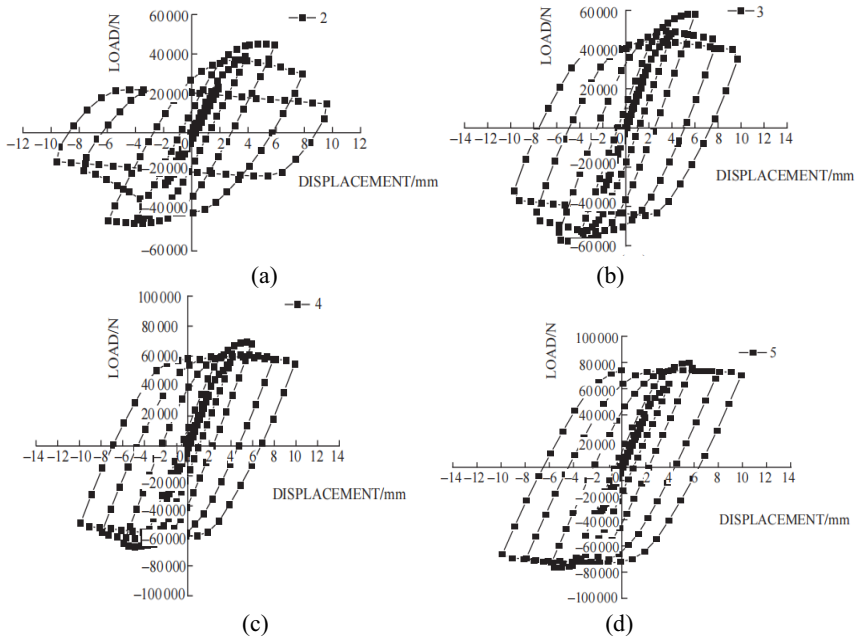


**Fig. 4.** Hysteresis curves for different steel pipe thicknesses (a) Hysteresis curve for 2 mm steel pipe thickness; (b) Hysteresis curve for 3 mm steel pipe thickness; (c) Hysteresis curve for 4 mm steel pipe thickness; (d) Hysteresis curve for 5 mm steel pipe thickness.

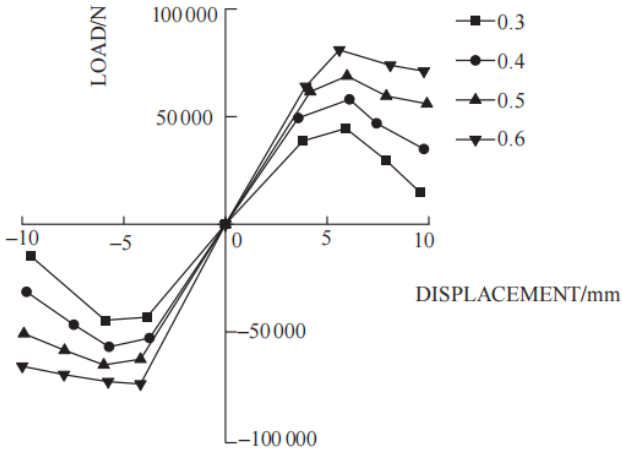


Fig. 5. Skeleton curves for different steel pipe thicknesses

## 4 Seismic Performance of Special-Shaped Column Frame Structure

### 4.1 Project Overview

The engineering design is for a 3-story frame structure with a total height and width of 9 meters each, resulting in a height-to-width ratio of 1. The structure is designed to withstand seismic intensity of degree 8. It falls under the first seismic group, class III site, with a design base earthquake acceleration peak of 0.20 g and a site characteristic period of 0.45 seconds. The structural damping ratio is 0.04, and it is classified as a category C building. For the steel tube concrete special-shaped column frame structure, the architectural structural analysis and design software ETABS is used for computational analysis. The component sizes are designed based on the existing results of parametric analysis of steel tube columns as per JGJ 149-2017 "Technical Specification for Concrete Special-shaped Column Structures" [12]. The structural plan layout is shown in Figure 6.

### 4.2 Modal Analysis Results

The results of modal analysis for each vibration mode of the frame structure are shown in Table 1. From Table 1, it is evident that the translational periods in the x and y directions are 0.820 seconds and 0.726 seconds, respectively, while the torsional deformation period is 0.647 seconds. The period ratio  $T_3/T_1 = 0.647/0.820 = 0.789$ , which is less than 0.85 and meets the regulatory requirement that the period ratio should not exceed 0.9. This indicates that the structure has considerable torsional stiffness, fulfilling the usage requirements.

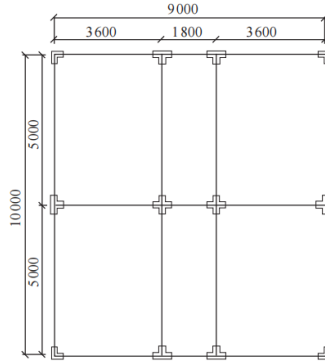


**Fig. 6.** Schematic of the Plan Layout of the Structural Model

**Table 1.** Modal Analysis Results

Mode Shape	Mode Shape	Period (s)
First Order Mode	Translational along y-axis	0.820
Second Order Mode	Translational along x-axis	0.726
Third Order Mode	Torsional Deformation	0.647

### 4.3 Time History Analysis

#### Selection of Earthquake Waves

Based on the damping ratio, characteristic period, and the periods of the first three modes from the modal analysis of the model structure, two simulated earthquake waves and five natural earthquake waves were selected using a MATLAB program. The comparison of these seven waves with the code-specified response spectrum is shown in Figure 7. The fitting of the code-specified response spectrum with the average response spectrum of the earthquake waves indicates that the selected earthquake waves are suitable for seismic calculation.

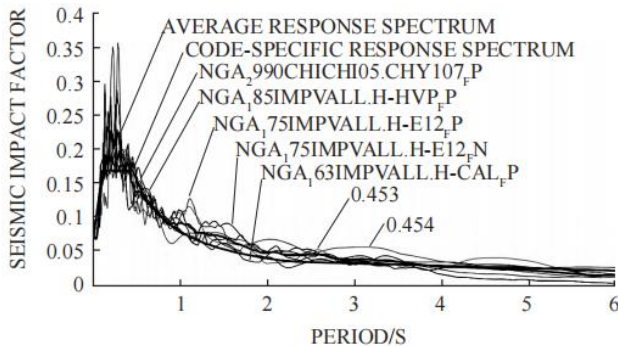


**Fig. 7.** Seismic Waves and Response Spectrum

### Frequently-Encountered Earthquake Time-History Analysis

Seismic waves are input into the ETABS model for a frequently-encountered earthquake time-history analysis. Among these, RG-1 and RG-2 are artificial waves, while TR-1, TR-2, TR-3, TR-4, and TR-5 are natural waves. Tables 2 and 3 compare the base shear of seismic waves with the base shear of the response spectrum. The results show that all are within the range of 80% to 120%, satisfying the code requirements of 65% to 135%. The average base shear ratio is 103.80% and 106.15%, meeting the code requirements of 80% to 120%.

**Table 2.** Comparison of Base Shear (x direction)

Earthquake Wave	Base Shear /kN	Earthquake Wave /RP-X
RP-X	385.2921	—
RG-1-X	403.823 2	104.81 %
RG-2-X	374.733 5	97.26 %
TR-1-X	423.811 2	110.00 %
TR-2-X	429.539 1	111.48 %
TR-3-X	395.971 9	102.77 %
TR-4-X	363.170 7	94.26 %
TR-5-X	408.556 4	106.04 %
Average		103.80 %

**Table 3.** Comparison of Base Shear (y direction)

Earthquake Wave	Base Shear /kN	Earthquake Wave /RP-X
RP-Y	347.968	-
RG-1-Y	369.162 2	106.09 %
RG-2-Y	380.461 9	109.34 %
TR-1-Y	371.072 1	106.64 %
TR-2-Y	393.950 1	113.21 %
TR-3-Y	329.167 8	94.60 %
TR-4-Y	337.360 4	96.95 %
TR-5-Y	404.324 6	116.20 %
Average		106.15 %

According to the GB 50011—2010 "Code for Seismic Design of Buildings" (2016 Edition), for an earthquake acceleration of 0.15g in an 8-degree zone, an acceleration of 70 cm/s<sup>2</sup> should be used for the time-history analysis of frequently encountered earthquakes. Tables 4 and 5 show the maximum inter-story displacements and maximum inter-story drift angles in the x and y directions of the structure under earthquake accelerations in U1 and U2 directions. The maximum inter-story drift angles in the x and y directions under the effect of the earthquake are less than 1/250, meeting the requirements.

### Rare Earthquake Elastic Analysis

According to the GB 50011—2010 "Code for Seismic Design of Buildings" (2016 Edition), for an earthquake acceleration of 0.2g in an 8-degree zone, an acceleration of 400 cm/s<sup>2</sup> should be used for the time-history analysis of rare earthquakes.



**Table 4.** Maximum Floor Displacement under Earthquake Action in the x Direction

Earthquake Wave	3rd Floor Displacement /mm	2nd Floor Displacement /mm	1st Floor Displacement /mm
RG-1-x	15.48	8.583	2.725
RG-2-x	15.755	8.718	2.785
TR-1-x	16.529	9.507	3.07
TR-2-x	15.044	8.661	2.828
TR-3-x	15.913	8.986	2.881
TR-4-x	13.74	7.702	2.431
TR-5-x	14.729	8.191	2.665

**Table 5.** Maximum Floor Displacement under Earthquake Action in the y Direction

Earthquake Wave	3rd Floor Displacement /mm	2nd Floor Displacement /mm	1st Floor Displacement /mm
RG-1-y	19.269	10.698	3.321
RG-2-y	18.88	10.46	3.235
TR-1-y	18.803	10.362	3.214
TR-2-y	17.84	10.017	3.178
TR-3-y	17.746	9.779	3.013
TR-4-y	14.201	8.008	2.556
TR-5-y	18.003	9.996	3.108

Tables 6 and 7 show the maximum inter-story displacements and the maximum inter-story drift angles in the x and y directions of the structure under earthquake accelerations in U1 and U2 directions. Under the effect of the earthquake, the maximum inter-story drift angles in both x and y directions are less than 1/50, meeting the requirements.

**Table 6.** Maximum Interlayer Displacement under Earthquake Action in the x Direction

Earthquake Wave	3rd Floor Displacement /mm	2nd Floor Displacement /mm	1st Floor Displacement /mm
RG-1-x	88.434	49.035	15.569
RG-2-x	89.814	49.69	15.874
TR-1-x	94.45	54.325	17.545
TR-2-x	86.411	49.747	16.243
TR-3-x	88.907	50.173	16.11
TR-4-x	78.792	44.175	13.84
TR-5-x	84.173	46.809	15.231

**Table 7.** Maximum Interlayer Displacement under Earthquake Action in the y Direction

Earthquake Wave	3rd Floor Displacement /mm	2nd Floor Displacement /mm	1st Floor Displacement /mm
RG-1-y	110.081	61.116	18.97
RG-2-y	108.166	59.93	18.535
TR-1-y	106.609	58.74	18.212
TR-2-y	101.395	56.916	18.056
TR-3-y	103.988	57.335	17.681
TR-4-y	81.514	45.966	14.67
TR-5-y	102.863	57.115	17.758

## 5 Conclusion

Through the use of ABAQUS and ETABS for component and overall structural seismic performance analysis of L-shaped steel pipe reinforced concrete special-shaped columns, the following conclusions can be drawn:

L-shaped steel pipe reinforced concrete special-shaped columns have good seismic performance. During the elastic deformation stage of the steel tube column, the change in axial compression ratio has no significant effect on it; however, when entering the elastoplastic deformation stage, the smaller the axial compression ratio, the better its seismic performance. Especially when the axial compression ratio is 0.3 or 0.4, the hysteresis curve is full, and no significant pinching phenomenon occurs, showing ideal seismic performance.

The change in the thickness of the external steel tube significantly affects the bearing capacity of the L-shaped steel pipe reinforced concrete special-shaped column. In the elastic deformation stage of the steel tube column, the thicker the external steel tube, the greater its ultimate bearing capacity; and when entering the elastoplastic deformation stage, the thicker the steel tube, the smoother its skeleton curve, showing better ductility.

Based on the actual conditions of rural buildings in Yunnan Province, an L-shaped steel pipe reinforced concrete special-shaped column structure model was established and calculated. The results show that the ratio of the third-order period to the first-order period of the structure is 0.789, less than 0.9; the maximum inter-story drift angles in the x direction ( $0^\circ$ ) and y direction ( $90^\circ$ ), as well as under bidirectional horizontal seismic action, are all less than 1/250; under frequent and rare earthquake actions in the x and y directions, the maximum inter-story drift angles of the model are within the specified range, meeting the requirements of GB 50011—2010 "Code for Seismic Design of Buildings" (2016 Edition).

Integrating the above results, the L-shaped steel pipe reinforced concrete column frame structure can safely and reliably meet the design code requirements when design parameters are reasonably selected. Due to its advantages such as high bearing capacity, good seismic performance, simple construction, and high assembly, L-shaped steel pipe reinforced concrete is suitable for widespread application in rural building construction.

## References

1. Hu X Y. (2018) Study on Seismic Performance of Square Steel Tube Reinforced Concrete Composite Special-Shaped Column Seismic Structure System [D]. Tianjin: Tianjin University. [https://kns.cnki.net/kcms2/article/abstract?v=5SxrylDe\\_PMTSB3fd3b-4FxfA\\_srcihg-CaUp705bBgDhRHEtCF6SBny7HMAsqUsb5YAKNJidmkkWD4Pd9Bhui4JMLx\\_w-JOcinACRbi9\\_k4FEt\\_RJrD9C\\_K7BZX6i\\_V5IkIxJb2Cw4uvi8g=&uniplatform=NZKPT&flag=copy](https://kns.cnki.net/kcms2/article/abstract?v=5SxrylDe_PMTSB3fd3b-4FxfA_srcihg-CaUp705bBgDhRHEtCF6SBny7HMAsqUsb5YAKNJidmkkWD4Pd9Bhui4JMLx_w-JOcinACRbi9_k4FEt_RJrD9C_K7BZX6i_V5IkIxJb2Cw4uvi8g=&uniplatform=NZKPT&flag=copy).
2. Zhou Y J. (2017) Seismic Performance Study of L-shaped Steel Pipe Reinforced Concrete Special-Shaped Columns Based on ABAQUS [D]. Tangshan: North China University of Science and Technology. [https://kns.cnki.net/kcms2/article/abstract?v=5SxrylDe\\_PNHxcNRV7K-9\\_EsxU2Ulg1FAiK61iSzUqxcC3fnhWW-\\_Emoqw\\_P6e3zd14\\_Z9jHVwsk\\_GC2\\_8M](https://kns.cnki.net/kcms2/article/abstract?v=5SxrylDe_PNHxcNRV7K-9_EsxU2Ulg1FAiK61iSzUqxcC3fnhWW-_Emoqw_P6e3zd14_Z9jHVwsk_GC2_8M)

- 7yb 9QLTI 9ZGXDc5 QQWJlE3 mgc0NOfnNpROYvnHG7biF4-eeU1osC 0BbJ Ub8A0=&uniplatform=NZKPT&flag=copy.
3. Zhang J. (2019) Earthquake Damage Analysis and Seismic Performance Study of L-shaped Steel Pipe Reinforced Concrete Columns [D]. Jingzhou: Yangtze University. [https://kns.cnki.net/kcms2/article/abstract?v=5SxrylDe\\_PN0kl4j-bDXuEM7j\\_x5p9\\_a7YqGb\\_-IUjnCJWQ\\_zIOSW\\_ZNHuO\\_HeRd\\_DoWUEbdJYUTMEIU4d7gD9m6OMmFF-V9Opc6QbqTd1qFo4xgkibHA8wIUf7kVmXImgR-A7wXgvdMqD-vyE=&uniplatform=NZKPT&flag=copy](https://kns.cnki.net/kcms2/article/abstract?v=5SxrylDe_PN0kl4j-bDXuEM7j_x5p9_a7YqGb_-IUjnCJWQ_zIOSW_ZNHuO_HeRd_DoWUEbdJYUTMEIU4d7gD9m6OMmFF-V9Opc6QbqTd1qFo4xgkibHA8wIUf7kVmXImgR-A7wXgvdMqD-vyE=&uniplatform=NZKPT&flag=copy).
  4. Zhao B Z. (2018) Study on Mechanical Performance of Square Steel Tube Reinforced Concrete Composite Special-Shaped Column Frame-Support Structure System [D]. Tianjin: Tianjin University. [https://kns.cnki.net/kcms2/article/abstract?v=5SxrylDe\\_PPW3\\_2TJx\\_Dqod9LkZ\\_Rd7ll8aOw-7PaQh\\_JphWX\\_dfFM\\_f3sAR\\_pfq0H\\_Z5c2\\_3jIQ\\_ZaAa\\_D7eM\\_mdfLr\\_WMCwT9pjXA0qxKSaMoCszaJ\\_J2Xtz\\_ZRNH\\_q4PCZa\\_zuelPu\\_lj1zjD\\_PnRj\\_ask=&uniplatform=NZKPT&flag=copy](https://kns.cnki.net/kcms2/article/abstract?v=5SxrylDe_PPW3_2TJx_Dqod9LkZ_Rd7ll8aOw-7PaQh_JphWX_dfFM_f3sAR_pfq0H_Z5c2_3jIQ_ZaAa_D7eM_mdfLr_WMCwT9pjXA0qxKSaMoCszaJ_J2Xtz_ZRNH_q4PCZa_zuelPu_lj1zjD_PnRj_ask=&uniplatform=NZKPT&flag=copy).
  5. Wang S. (2020) Seismic Performance Study of Prefabricated Steel Pipe Reinforced Concrete Special-Shaped Column Side Frame [D]. Tangshan: North China University of Science and Technology. [https://kns.cnki.net/kcms2/article/abstract?v=5SxrylDe\\_PO-Hyl3sOU7t3D8OS\\_-hyb8\\_sFz7KcRptDfls0gjNobEmm\\_7s57XS\\_02LlJi\\_UFxfjM\\_mxnS\\_a8z91pMrOiJzW66KAtADdE1D5ut7P2HdVNnjxDxU4TftNnJlyJPVnAkFetTon7\\_hA=&uniplatform=NZKPT&flag=copy](https://kns.cnki.net/kcms2/article/abstract?v=5SxrylDe_PO-Hyl3sOU7t3D8OS_-hyb8_sFz7KcRptDfls0gjNobEmm_7s57XS_02LlJi_UFxfjM_mxnS_a8z91pMrOiJzW66KAtADdE1D5ut7P2HdVNnjxDxU4TftNnJlyJPVnAkFetTon7_hA=&uniplatform=NZKPT&flag=copy).
  6. Montuori R ,Nastri E ,Piluso V , et al. (2024) Experimental and analytical study on the behaviour of circular concrete filled steel tubes in cyclic bending[J].*Engineering Structures*,2024,304117610-.DOI:10.1016/J.ENGSTRUCT.2024.117610.
  7. Bhat P, Jamatia R. (2024) Compressive behavior of concrete-filled double skin steel tubular columns: An analytical approach[J]. *Journal of Constructional Steel Research*,2024, 214108483-.DOI: 10.1016/J.JCSR.2024.108483.
  8. Dai B H,Tao Z, Xu G L, et al. (2021) Investigation of Earthquake Damage to Rural Houses in the Epicentral Area of the M<sub>s</sub>6.4 Yangbi Earthquake [J]. *World Earthquake Engineering*, 37(3):9–18. DOI: 10.3969/j.issn.1007-6069.2021.03.002.
  9. Dai B H, Tao Z, WAHAB, et al. (2022) Investigation and Analysis of Earthquake Damage to Rural Houses in the Ninglang 5.5 Earthquake [J]. *Journal of Natural Disasters*, 31(2): 48–55. DOI: 10.3969/j.issn.1001-8662.2002.04.002.
  10. Zhong S T. (2003) *Steel Pipe Reinforced Concrete Structures* [M]. Beijing: Tsinghua University Press. <https://www.guifanku.com/tushushouce/672089.html>.
  11. Han L H. (2000) *Steel Pipe Reinforced Concrete Structures* [M]. Beijing: Science Press. <https://www.guifanku.com/tushushouce/602959.html>.
  12. Technical Regulations for Concrete Special-Shaped Column Structures: JGJ 149—2017[S]. <https://www.guifanku.com/zykszl/704563.html>.

**Open Access** This chapter is licensed under the terms of the Creative Commons Attribution-NonCommercial 4.0 International License (<http://creativecommons.org/licenses/by-nc/4.0/>), which permits any noncommercial use, sharing, adaptation, distribution and reproduction in any medium or format, as long as you give appropriate credit to the original author(s) and the source, provide a link to the Creative Commons license and indicate if changes were made.

The images or other third party material in this chapter are included in the chapter's Creative Commons license, unless indicated otherwise in a credit line to the material. If material is not included in the chapter's Creative Commons license and your intended use is not permitted by statutory regulation or exceeds the permitted use, you will need to obtain permission directly from the copyright holder.

